Universal crossing of the self-avoiding walk critical exponent nu at the Euclidean value 3/4 for several different fractal families

# Universal crossing of the self-avoiding walk critical exponent ν at the Euclidean value 3/4 for several different fractal families

Sava Milošević† and Ivan Živić‡

† Faculty of Physics, University of Belgrade, P O Box 550, 11001 Belgrade, Serbia, Yugoslavia
‡ Faculty of Natural Sciences and Mathematics, The Svetozar Marković University, 34000 Kragujevac, Serbia, Yugoslavia

**Abstract.** We find that the end-to-end distance critical exponent $\nu$ is close to the Euclidean value 3/4 for self-avoiding walks (SAWs) on fractals that are composed of homogeneous parts of size $b_h \approx 26$. More precisely, we find that SAWs on fractals with smaller homogeneous parts ($b < 25$) have $\nu > 3/4$, while $\nu < 3/4$ on fractals with $b > 27$. We establish this result in the case of three quite different fractal families: the Sierpinski gasket (SG) family, the plane-filling (PF) family, and the checkerboard (CB) family of fractals. In the case of the first two families (SG and PF), the relevant values for $\nu$ were found previously by applying the Monte Carlo renormalization group (MCRG) method, but the specific value $b_h$ was not recognized. On the other hand, for the CB fractals only the exact renormalization group (RG) results were known previously (for $3 \leqslant b \leqslant 9$, where $b$ is an odd integer that serves as the fractal enumerator). In this paper we extend the sequence of the known results for the CB family up to $b = 81$ by generalizing the MCRG method. The new results have revealed the occurrence of the aforementioned crossing of the Euclidean value 3/4. We discuss the significance of the crossing within the current knowledge of SAWs on fractals.

## 1. Introduction

Recent investigations of self-avoiding walks (SAWs) on the Sierpinski-gasket (SG) family of fractals [1,2], and on the plane-filling (PF) family [3], revealed that the critical exponent $\nu$ (associated with the mean-squared end-to-end distance) can be larger as well as smaller than 3/4, which is the value predicted for two-dimensional Euclidean lattices. Members of the SG family can be enumerated by an integer $b$ ($2 \leqslant b < \infty$), while members of the PF family can be enumerated by the odd integer $b \geqslant 3$. It was interesting to observe that in both cases (for the studied intervals $2 \leqslant b \leqslant 80$ and $3 \leqslant b \leqslant 121$ for the SG and PF families, respectively) $\nu$ displayed a kind of monotonic decrease with $b$ and, more interestingly, it crossed the value 3/4 at $b \approx 27$ in both cases. This may have appeared as a peculiarity of the two families studied, since no similar cases are known. In particular, the exact renormalization group (RG) study [4] of SAWs on the first four members of the checkerboard (CB) family of fractals did not indicate that $\nu$ as a function of the corresponding fractal enumerator $b$ (an odd number, $3 \leqslant b < \infty$) could behave in the same way. However, in this paper we apply the Monte Carlo renormalization group (MCRG) method to study SAWs on the CB fractals for $3 \leqslant b \leqslant 81$ and demonstrate that $\nu$ displays the same type of behaviour in the region close to $b \approx 25$. Therefore, we can say that in all three cases the critical exponent $\nu$ crosses the

Euclidean value in a very narrow region of $b$ ($25 \leqslant b \leqslant 27$), that is, for fractals which have homogeneous parts of a particular size $b_h \approx 26$. To our knowledge, this is the first kind of universality observed for SAWs on fractals. This finding explains, for instance, certain results related to the controversial problem of SAWs on the critical percolation clusters.

The MCRG method used in this paper to get values of $\nu$ for SAWs on CB fractals is based on the approach applied in the case of SG [2] and PF [3] fractals. It is not a straightforward generalization of the MCRG approaches [2] and [3] that could work in the case of CB fractals. Indeed, in this case one needs three parameters [4] to formulate an appropriate exact renormalization group (RG), which makes the corresponding Monte Carlo (MC) simulations more complex. We have found means to handle this complexity in such a way that the obtained MCRG results deviate by at most 0.06% from the limited set of available exact results [4]. Details of the present MCRG approach are given in the next section. In addition, in section 2 we shall describe the CB family of fractals and introduce the requisite RG parameters for studying SAWs on these fractals. In section 3 we present the obtained results and discuss their significance within the framework of the current knowledge of the properties of SAWs on fractals.

## 2. The three-parameter Monte Carlo renormalization group

Each member of the CB family of fractals is labelled by an odd integer $b \geqslant 3$ and can be obtained as the result of an infinite iterative process of successively enlarging the fractal structure $b$ times and replacing the smallest parts of the enlarged structure with the generator (initial structure). The generator of a CB fractal is a square, of size $b \times b$, composed of $b$ rows of unit squares, so that within each row and each column every other of them is removed (see figure 1). Thus, the $b = 3$ fractal appears to be equivalent to the Vicsek snowflake fractal [5], whereas the $b = \infty$ fractal generator appears to be a $\pi/2$ wedge of square lattice. The fractal dimension $d_f$ for an arbitrary member specified by $b$ can be easily found to be $\ln[(b^2 + 1)/2]/\ln b$. On the other hand, the spectral dimension $d_s$ can be deduced, for $b = 3$ and $b = 5$, from the known data [6] for the resistivity of the corresponding electrical networks ($d_s = 1.18863$ and $d_s = 1.30161$ for $b = 3$ and $b = 5$, respectively), while for $b \geqslant 7$ a similar calculation of the resistivity turns out to be formidable. For increasing $b$, one can expect that members of the CB family become more and more similar to the ordinary square lattice, which is indicated by the fact that the fractal dimension $d_f$ tends to 2 when $b \to \infty$.
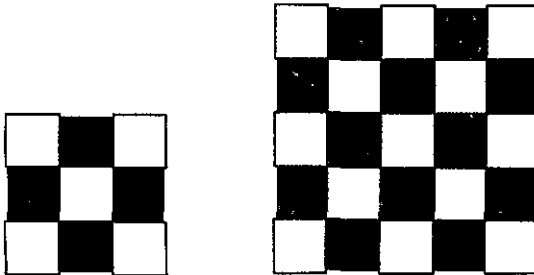


**Figure 1.** The fractal generators of the first two members, $b = 3$ and $b = 5$, of the checkerboard (CB) family of fractals. The black squares do not belong to the generators and, accordingly, they are not available for SAWs.

The critical exponent $\nu$ describes the scaling law $\langle R_N^2 \rangle \sim N^{2\nu}$ for the mean squared end-to-end distance for $N$-step SAWs (assuming that $N$ is very large). We can calculate this critical exponent in the framework of the RG method [4], in which we consider the $r$th-stage fractal structure lattice (that can be obtained after the $r$th step of the iterative construction of the entire fractal) and introduce the three restricted partition functions

$$F^{(r)}(x) = \sum_N F_N x^N \tag{1}$$

$$G^{(r)}(x) = \sum_N G_N x^N \tag{2}$$

$$H^{(r)}(x) = \sum_N H_N x^N \tag{3}$$

where $x$ is the weight factor (fugacity) for each elementary step of the SAW and $F_N$ is the number of all possible $N$-step SAWs that start at one corner and end at the nearest corner of an $r$th-stage fractal structure (see figure 2). Similarly, $G_N$ in (2) is the number of $N$-step SAWs that start at one corner and end at the diagonally opposite corner of the $r$th-stage fractal structure, and $H_N$ is the number of $N$-step SAWs that consist of two non-intersecting SAW parts, such that each of them starts at one corner and ends at one of two nearest corners of the $r$th-stage fractal structure (see figure 2).
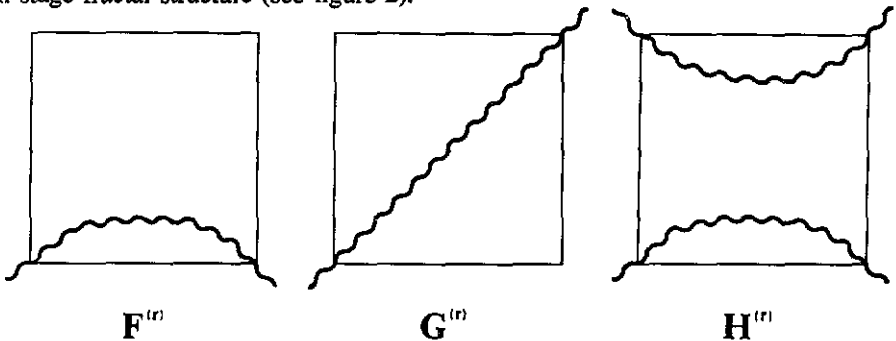


**Figure 2.** Schematic representation of the three restricted partition functions (for an $r$th-stage fractal structure) used in the calculation of the SAW critical exponent $\nu$. The interior details of the $r$th-order fractal structure is not shown (it is manifested by the wiggles of the SAW paths).

The recursive nature of the fractal construction implies the following recursion relation,

$$F^{(r+1)} = \sum_{N_F, N_G, N_H} f_{N_F, N_G, N_H} \left( F^{(r)} \right)^{N_F} \left( G^{(r)} \right)^{N_G} \left( H^{(r)} \right)^{N_H} \tag{4}$$

for the restricted partition function $F$, and quite similar relations for the restricted partition functions $G$ and $H$. Because of the underlying self-similarity, the corresponding set of relations does not depend on the particular stage of fractal construction. For this reason, the coefficients $f_{N_F, N_G, N_H}$ are not functions of $r$. Each of them represents the number of ways in which the corresponding part of the SAW path, within the $(r + 1)$th-stage fractal structure, can be comprised of all three types of the SAW paths within the fractal structures of the next lower order. Consequently, $f_{N_F, N_G, N_H}$ represents the number of ways in which the $F$ type of SAWs (see figure 2), within the $(r + 1)$th-stage of fractal structure, can be constructed so that it contains $N_F$, $N_G$ and $N_H$ parts, respectively, of the $F$, $G$ and $H$ type

of SAWs within the comprising $r$th stages of fractal construction (specific values of these coefficients, for $b = 5$ and $b = 7$, can be found in [4]).

The set of relations of the type (4) can be considered as the RG transformations for the SAW problem under study (in what follows, we shall use the prime symbol as a superscript for the $(r + 1)$th-order parameters and no indices for the $r$th-order parameters). In order to find the critical exponent $\nu$, we should determine the non-trivial fixed point of these transformations, and then we should solve the corresponding eigenvalue problem of the linearized RG transformations, that is, we should solve the equation

$$
\begin{vmatrix}
\left(\dfrac{\partial F'}{\partial F} - \lambda\right) & \dfrac{\partial F'}{\partial G} & \dfrac{\partial F'}{\partial H} \\[2mm]
\dfrac{\partial G'}{\partial F} & \left(\dfrac{\partial G'}{\partial G} - \lambda\right) & \dfrac{\partial G'}{\partial H} \\[2mm]
\dfrac{\partial H'}{\partial F} & \dfrac{\partial H'}{\partial G} & \left(\dfrac{\partial H'}{\partial H} - \lambda\right)
\end{vmatrix}^{*} = 0
\tag{5}
$$

where the asterisk means that all derivatives should be taken at the fixed point. Knowing the relevant eigenvalue, which we denote by $\lambda_1$, we can determine the critical exponent $\nu$ using the formula

$$
\nu = \frac{\ln b}{\ln \lambda_1(b)}.
\tag{6}
$$

To learn a specific value of $\nu$, for a given $b$, one should first find the coefficients $f_{N_F, N_G, N_H}$ and the corresponding coefficients for the functions $G$ and $H$. However, finding exact values of these coefficients requires an enormous amount of computer work, which has been so far performed only for $b \leqslant 9$ [4]. Thus, to get an entire sequence of values of $\nu$ for $b \geqslant 11$, we are going to circumvent the problem of finding the exact coefficients in the RG equations by applying the MCRG technique.

The MCRG method, if properly applied, allows us to find directly the derivatives that appear in the eigenvalue equation (5). It starts by locating the non-trivial fixed point, which requires, at the beginning, an implementation of the MC simulation of the SAWs for a chosen initial set of values $(F_0, G_0, H_0)$. In other words, we let the walker start its walking, for instance, at the lower left corner of the fractal generator and record the corner at which it leaves the generator, together with recording the total numbers $N_F$, $N_G$ and $N_H$ of crossings of the $F$, $G$ or $H$ type (see figure 2) through elementary squares. The SAW walker crosses an elementary square in the $F$, $G$ or $H$ way with the weight (probability) $F_0$, $G_0$ and $H_0$, respectively. We repeat this MC simulation $L$ times, for the same set $(F_0, G_0, H_0)$, and thus we find how many times the walker has passed through the generator in the $F$, $G$ or $H$ way. We then get the values $F'(F_0, G_0, H_0)$, $G'(F_0, G_0, H_0)$ and $H'(F_0, G_0, H_0)$ by dividing the corresponding numbers by $L$. In this way we complete the first step of our generalization of the 'homing' procedure [7] for determining the relevant fixed point. In the next step, instead of using the unknown complete RG equations of type (4), we invoke the expansion

$$
\begin{aligned}
F'(F, G, H) \approx\ & F'(F_0, G_0, H_0) \\
& + \left.\frac{\partial F'}{\partial F}\right|_0 (F - F_0) + \left.\frac{\partial F'}{\partial G}\right|_0 (G - G_0) + \left.\frac{\partial F'}{\partial H}\right|_0 (H - H_0) \\
& + \frac{1}{2}\left.\frac{\partial^2 F'}{\partial F^2}\right|_0 (F - F_0)^2 + \frac{1}{2}\left.\frac{\partial^2 F'}{\partial G^2}\right|_0 (G - G_0)^2 + \frac{1}{2}\left.\frac{\partial^2 F'}{\partial H^2}\right|_0 (H - H_0)^2
\end{aligned}
$$

$$+ \frac{\partial^2 F'}{\partial F \partial G}\Big|_0 (F - F_0)(G - G_0) + \frac{\partial^2 F'}{\partial F \partial H}\Big|_0 (F - F_0)(H - H_0)$$

$$+ \frac{\partial^2 F'}{\partial G \partial H}\Big|_0 (G - G_0)(H - H_0) \tag{7}$$

and similar expansions for $G'(F, G, H)$ and $H'(F, G, H)$. In these expansions, all quantities on the right-hand sides can be determined through the MC simulations. Indeed, the way we obtain the first terms in such expansions has already been explained, while the derivatives at the point $(F_0, G_0, H_0)$ can be related to various averages of $N_F$, $N_G$ and $N_H$. For instance, starting with (4) (in the notation that does not use the superscripts $(r + 1)$ and $r$) and by differentiating it with respect to $F$ we get

$$\frac{\partial F'}{\partial F} = \sum_{N_F, N_G, N_H} N_F f_{N_F, N_G, N_H}(F)^{N_F - 1}(G)^{N_G}(H)^{N_H}. \tag{8}$$

Treating now $F'$ as the grand canonical partition function, for the ensemble of all possible SAWs that start at the lower left corner of the fractal generator and leave it at the lower right corner, we can write the corresponding ensemble average

$$\langle N_F(F, G, H)\rangle_{F'} = \frac{1}{F'} \sum_{N_F, N_G, N_H} N_F f_{N_F, N_G, N_H}(F)^{N_F}(G)^{N_G}(H)^{N_H} \tag{9}$$

which can be directly measured in an MC simulation. Finally, comparing the last two equations, we can express one of the requisite derivatives in terms of the measurable quantity

$$\frac{\partial F'}{\partial F} = \frac{F'}{F}\langle N_F(F, G, H)\rangle_{F'}. \tag{10}$$

In a similar way, one can get additional eight derivatives, so that we can write the general formula

$$\frac{\partial Y'}{\partial X} = \frac{Y'}{X}\langle N_X \rangle_{Y'} \tag{11}$$

where $X$ and $Y$ stand for any pair of quantities from the set $\{F, G, H\}$. Accordingly, the second derivatives that appear in (7) and likewise, expansions for $G'(F, G, H)$ and $H'(F, G, H)$, can be obtained by differentiating (11) with respect to Z, where $Z \in \{F, G, H\}$. The result can be written in a condensed form

$$\frac{\partial^2 Y'}{\partial Z \partial X} = \frac{Y'}{XZ}\left(\langle N_Z N_X\rangle_{Y'} - \frac{\partial X}{\partial Z}\langle N_X\rangle_{Y'}\right) \tag{12}$$

which can be further simplified as

$$\frac{\partial^2 Y'}{\partial X^2} = \frac{Y'}{X^2}\left(\langle N_X^2\rangle_{Y'} - \langle N_X\rangle_{Y'}\right) \tag{13}$$

for $X = Z$ and as

$$\frac{\partial^2 Y'}{\partial Z \partial X} = \frac{Y'}{XZ}\langle N_Z N_X\rangle_{Y'} \tag{14}$$

for $X \neq Z$. In the last two formulae, the quantities $\langle N_X^2 \rangle_{Y'}$ and $\langle N_Z N_X \rangle_{Y'}$ can be measured in an MC simulation, as well as the quantity $\langle N_X \rangle_{Y'}$.

The preceding paragraph outlines the essence of the generalized 'homing' procedure. Yet, its last stage should be explained with an additional care. Namely, starting with the initial set $(F_0, G_0, H_0)$ and after performing an MC simulation, one looks for the fixed point by solving numerically equations of the type (7). The solution, denoted by $(F_1, G_1, H_1)$, can be accepted to be a good approximation for the exact fixed point if the differences between the respective values of $(F_1, G_1, H_1)$ and $(F_0, G_0, H_0)$ are small enough. More precisely, one should require

$$|F_1 - F_0| < \Delta F_0 \qquad |G_1 - G_0| < \Delta G_0 \qquad |H_1 - H_0| < \Delta H_0 \qquad (15)$$

where $\Delta F_0$, $\Delta G_0$ and $\Delta H_0$ are the inherent uncertainties of the method applied. However, the latter quantities cannot be unambiguously specified (in contrast with the one-parameter MCRG method [2, 7]) even though, in principle, they can be determined from

$$\Delta F_0' = \frac{\partial F'}{\partial F}\bigg|_0 \Delta F_{0F} + \frac{\partial F'}{\partial G}\bigg|_0 \Delta G_{0F} + \frac{\partial F'}{\partial H}\bigg|_0 \Delta H_{0F} \qquad (16)$$

and from two similar equations for $\Delta G_0'$ and $\Delta H_0'$ by taking, for instance, $\Delta F_0 = \text{Max}(\Delta F_{0F}, \Delta F_{0G}, \Delta F_{0H})$. Unfortunately, the increments on the right-hand sides of above equations are not directly measured, whereas $\Delta F_0'$, $\Delta G_0'$ and $\Delta H_0'$ are measurable quantities, as well as the pertinent nine partial derivatives. In this situation, we assume, in each of the equations of the type (16), equal contributions of the corresponding three terms, and thereby we adopt the following convention for finding the requisite uncertainties

$$\Delta X_0 = \text{Max} \left( \frac{\Delta F_0'}{3\frac{\partial F'}{\partial X}\big|_0}, \frac{\Delta G_0'}{3\frac{\partial G'}{\partial X}\big|_0}, \frac{\Delta H_0'}{3\frac{\partial H'}{\partial X}\big|_0} \right) \qquad (17)$$

where $X \in \{F, G, H\}$. In this way we specify conditions (15). If it turns out that these conditions are not satisfied, we accept the set $(F_1, G_1, H_1)$ as the next initial set of values and repeat the described MC procedure. Of course, in practice, it is usually necessary to repeat this procedure $n$ times until the conditions

$$|F_n - F_{n-1}| < \Delta F_{n-1} \qquad |G_n - G_{n-1}| < \Delta G_{n-1} \qquad |H_n - H_{n-1}| < \Delta H_{n-1} \qquad (18)$$

become satisfied, so that finally the fixed point is identified with $(F_n, G_n, H_n)$, which completes the 'homing' procedure.

Having determined the fixed point, we need to solve the eigenvalue equation (5) in order to find the critical exponent $\nu$ via the formula (6). Thus, we should find the partial derivatives $\partial Y'/\partial X$ (where $X, Y \in \{F, G, H\}$) at the fixed point, that is, at the point $(F_n, G_n, H_n) \equiv (F^*, G^*, H^*)$ (it should be pointed out that the last MC simulation provides data for the partial derivatives at the point $(F_{n-1}, G_{n-1}, H_{n-1})$, but not at the fixed point). To this end, we use the expansion

$$\langle N_X \rangle_{Y'}^* = \langle N_X \rangle_{Y'} \bigg|_{n-1} + \frac{\partial \langle N_X \rangle_{Y'}}{\partial F}\bigg|_{n-1} (F^* - F_{n-1})$$
$$+ \frac{\partial \langle N_X \rangle_{Y'}}{\partial G}\bigg|_{n-1} (G^* - G_{n-1}) + \frac{\partial \langle N_X \rangle_{Y'}}{\partial H}\bigg|_{n-1} (H^* - H_{n-1}) \qquad (19)$$

where the partial derivatives at the point $(F_{n-1}, G_{n-1}, H_{n-1})$ can be calculated using the formula

$$\frac{\partial \langle N_X \rangle_{Y'}}{\partial F} = \frac{1}{F}\left(\langle N_F N_X \rangle_{Y'} - \langle N_F \rangle_{Y'} \langle N_X \rangle_{Y'}\right) \tag{20}$$

and similar formulae for $\partial\langle N_X \rangle_{Y'}/\partial G$ and $\partial\langle N_X \rangle_{Y'}/\partial H$ that follow from relations of the type (9). These formulae contain only the quantities that are directly measurable. In this way we can learn, through the MC simulations, the partial derivatives that appear in the eigenvalue equation (5), and consequently we can solve this equation numerically. It turns out that in all cases under study ($5 \leqslant b \leqslant 81$) the latter equation has only one relevant eigenvalue ($\lambda_1 > 1$).

## 3. Results and discussion

In this section we present our MCRG results for the SAW critical exponent ν for the CB family of fractals and discuss their relevance to the current knowledge of SAWs on fractals. We begin with presenting specific results for the coordinates of the fixed point $(F^*, G^*, H^*)$ and ν for $5 \leqslant b \leqslant 81$. These data are given in table 1 together with the exact RG results for $3 \leqslant b \leqslant 9$ [4]. First, we note that there is very good agreement between the MCRG results for ν and the corresponding exact RG results, that is, no deviation is larger than 0.06%. This means that, in spite of the complexity of performed calculations, the deviations for ν are of the same order of magnitude as those found in the case of the one-parameter MCRG calculations [2,3]. Next, we observe the monotonic decrease of ν when b increases and, in particular, the crossing of the Euclidean value $\nu = 0.75$ at $b \approx 25$.

**Table 1.** The MCRG ($5 \leqslant b \leqslant 81$) results obtained in this work for the fixed-point parameters $F^*$, $G^*$ and $H^*$, and the SAW critical exponent ν. For the sake of comparison, we also give the corresponding exact RG results [4], for $3 \leqslant b \leqslant 9$.

| b | No of MC realization | $F^*$ | $G^*$ | $H^*$ | ν |
|---|---|---|---|---|---|
| 3 | exact | | 1 | | 1.00000 |
| 5 | exact | 0.66371 | 0.72464 | 0.10003 | 0.85235 |
| | $10^5$ | $0.66433 \pm 0.00058$ | $0.72433 \pm 0.00047$ | $0.10003 \pm 0.00510$ | $0.85216 \pm 0.00304$ |
| 7 | exact | 0.56805 | 0.62296 | 0.05849 | 0.81502 |
| | $10^5$ | $0.56783 \pm 0.00040$ | $0.62328 \pm 0.00043$ | $0.05729 \pm 0.00267$ | $0.81552 \pm 0.00199$ |
| 9 | exact | 0.51576 | 0.57123 | 0.03869 | 0.79578 |
| | $10^5$ | $0.51482 \pm 0.00034$ | $0.57236 \pm 0.00041$ | $0.03819 \pm 0.00326$ | $0.79594 \pm 0.00167$ |
| 11 | $10^5$ | $0.48460 \pm 0.00028$ | $0.53776 \pm 0.00037$ | $0.02927 \pm 0.00277$ | $0.78338 \pm 0.00142$ |
| 13 | $1.1 \times 10^5$ | $0.46113 \pm 0.00024$ | $0.51878 \pm 0.00033$ | $0.02156 \pm 0.00333$ | $0.77532 \pm 0.00124$ |
| 15 | $10^5$ | $0.44802 \pm 0.00024$ | $0.49998 \pm 0.00035$ | $0.01672 \pm 0.00285$ | $0.76850 \pm 0.00115$ |
| 19 | $10^5$ | $0.42743 \pm 0.00021$ | $0.47866 \pm 0.00031$ | $0.01041 \pm 0.00235$ | $0.75980 \pm 0.00098$ |
| 23 | $10^5$ | $0.41627 \pm 0.00020$ | $0.46245 \pm 0.00031$ | $0.00783 \pm 0.00315$ | $0.75261 \pm 0.00092$ |
| 25 | $10^5$ | $0.41088 \pm 0.00019$ | $0.45764 \pm 0.00030$ | $0.00648 \pm 0.00234$ | $0.75002 \pm 0.00086$ |
| 27 | $10^5$ | $0.40912 \pm 0.00018$ | $0.44998 \pm 0.00028$ | $0.00565 \pm 0.00335$ | $0.74756 \pm 0.00084$ |
| 35 | $10^5$ | $0.39741 \pm 0.00018$ | $0.43778 \pm 0.00026$ | $0.00380 \pm 0.00535$ | $0.74221 \pm 0.00082$ |
| 43 | $1.3 \times 10^5$ | $0.39479 \pm 0.00013$ | $0.42344 \pm 0.00020$ | $0.00271 \pm 0.00318$ | $0.73742 \pm 0.00060$ |
| 51 | $10^5$ | $0.39211 \pm 0.00021$ | $0.41537 \pm 0.00033$ | $0.00143 \pm 0.00613$ | $0.73371 \pm 0.00079$ |
| 61 | $10^5$ | $0.38865 \pm 0.00018$ | $0.40980 \pm 0.00028$ | $0.00095 \pm 0.00451$ | $0.73196 \pm 0.00067$ |
| 71 | $10^5$ | $0.38835 \pm 0.00011$ | $0.40280 \pm 0.00017$ | $0.00082 \pm 0.00187$ | $0.72910 \pm 0.00050$ |
| 81 | $10^5$ | $0.38686 \pm 0.00017$ | $0.39970 \pm 0.00027$ | $0.00076 \pm 0.00148$ | $0.72765 \pm 0.00056$ |

In figure 3 we depict the SAW critical exponent $\nu$, for the CB fractals, as a function of $1/b$. In this figure we also present data for the SG [2] and the PF [3] families of fractals. One can see that all three sets of data represent monotonically decreasing functions of $b$ whose last values, in the intervals under study, lie well below the Euclidean value $\nu = 3/4$. Details of further behaviour of these three functions are unknown, except for the finite-size scaling argument [3,8] for the PF and SG fractals which in both cases predicts that $\nu$ approaches 3/4 from *below* when $b \rightarrow \infty$. One could expect similar behaviour in the case of CB fractals, but the pertinent finite-size scaling argument cannot be elaborated since the requisite scaling laws for the functions $F$, $G$ and $H$, are unknown, although our findings provide certain knowledge about them. For instance, one can see from table 1 that values of $H^*$ decrease much faster than values for $F^*$ and $G^*$, in such a way that one can expect that $H^*$ vanishes for very large $b$ and, for this reason, it could be neglected in the corresponding finite-size scaling argument. This type of behaviour of $H^*$ can be related to the meaning of the partition function $H$ (see figure 2) within the ensemble of all possible walks, whereby it should be clear that probability of the $H$ type of SAWs vanishes for very large fractal generators.

In addition to the foregoing technical details, one can rightfully raise the question about the apparent dichotomy between the observed decrease of data for finite $b$ (in all three cases) and the predicted increase of data in the asymptotic region $b \rightarrow \infty$, where they are expected to start to converge to 3/4 *from below* [8]. At the beginning, one should notice that this dichotomy would have appeared even if we had not applied our MCRG. The dichotomy was brought about by the exact RG results for $\nu$ for the SG fractals [1] and by the subsequent finite-size scaling arguments [8], and it was later corroborated by a similar study in the case of PF fractals [3]. Moreover, the dichotomy is something that springs from various phenomenological formulae for $\nu$ [9–14] when they are applied to the fractals studied. Under these circumstances, the MCRG results for $\nu$ have made a step forward by demonstrating that the dichotomous behaviour of $\nu$ is not a peculiarity of the SG fractals, and, more importantly, by settling an important part of the dichotomy. Indeed, if the two predictions for the two regions of $b$ (one for small $b$ and the other for very large $b$) are both correct and the data for $\nu$ are to meet somewhere, then the data should *first* cross the 3/4 value at some finite $b$, which has been vindicated by the MCRG approach. In addition, the data should exhibit a minimum at some finite (but probably very large) $b$. Unfortunately, the MCRG results obtained so far do not seem to be close to the position of the expected minimum. In fact, none of the phenomenological formulae [9–14] predicts a minimum before $b = 650$ in the case of the SG fractals [2], while a generalization of the approach initiated in [9] predicts the earliest location of the minimum at $b \approx 1800$ [3,15], that is, in a region that can hardly be reached using the present-day computers. This makes the entire problem more tantalizing, in particular as it seems not to be isolated. For instance, the systematic decrease below the relevant Euclidean value was observed also in the case of the crossover exponent $\phi$ for polymer adsorption on the SG fractals [16].

Finally, we come back to the crossing of the Euclidean value $\nu = 3/4$ (see figure 3) that happens very close to $b_h = 26$, in the case of all three families of fractals (SG, PF and CB). The closeness of the three crossings is surprising (it could not have been expected on the grounds of the corresponding exact RG results obtained for $b < 10$). Precisely, the three families comprise fractals of very different appearances and, more importantly, with different characteristics, that is, with disparate fractal $d_f$ and spectral $d_s$ dimensions (for instance, $d_f = 2$ for the entire PF family, whereas for both SG and CB $d_f$ is given by two different monotonically increasing functions of $b$ which approach 2 only for $b \rightarrow \infty$). Furthermore, it is appropriate to point out here that results obtained for the CB family of
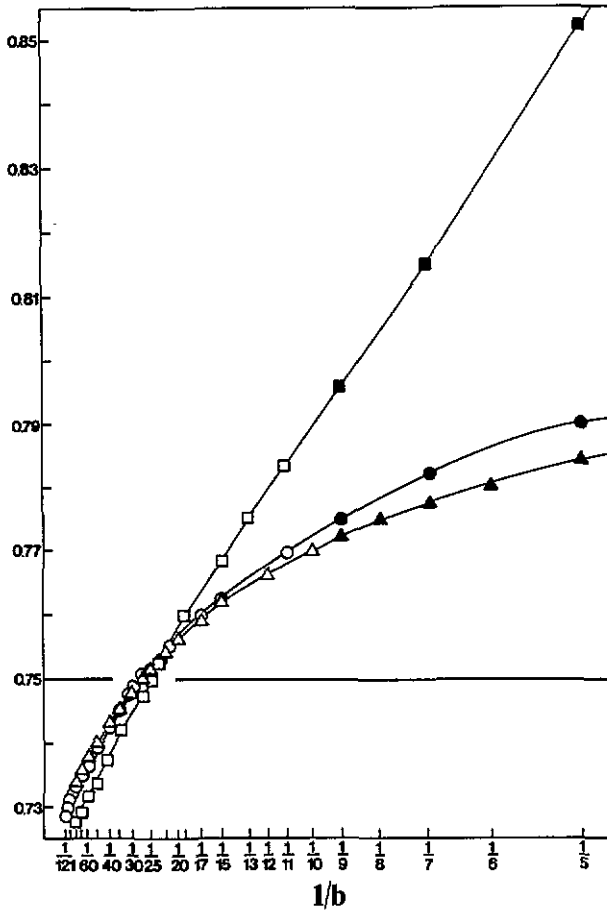
**Figure 3.** Data for the SAW critical exponent $v$ for the SG family of fractals ($\triangle$ and $\blacktriangle$), PF family ($\bigcirc$ and $\bullet$) and CB family ($\square$ and $\blacksquare$), plotted as functions of $1/b$. The exact RG results are represented by solid symbols ($\blacktriangle$, $\bullet$ and $\blacksquare$), while the MCRG results are depicted by open symbols. The thin lines that connect the results, serve merely as guides to the eye. The solid horizontal line represents the Euclidean value 3/4. In the case of the CB data, there is an inflection for $b < 25$ (see figure 4 of reference [4]), which might cause an impression that there is a fault in the data. However, error bars related to the MCRG data in all three cases (SG, PF and CB) are so small that they all lie within the corresponding symbols. It is worth noting that there is no other simple function of $b$ (of the type $1/b^x$, where $x$ is a constant, or of the type $1/\ln b$) which makes the three *entire sets* of data mutually separated and, to some extent, parallel. The notable exception may be the plot of $v$ versus the spectral dimension $d_s$ (see figure 5 of reference [3]), but, unfortunately, $d_s$ is not known for the CB fractals for $b > 5$.

fractals are valid also for the family of X fractals [4]. Thus, the only common feature in the region where the crossing of the Euclidean value 3/4 takes place appears to be the fact that the corresponding fractals have *homogeneous pieces* of the same size $b_h \times b_h$. Since our MCRG results deviate very little (at most 0.06% in all three cases) from the available exact RG results, one can accept the crossing as a reliable finding relevant to SAWs on fractals. In fact, this is, to our knowledge, the first universal element in the case of SAWs on fractals

and as such it should be further scrutinized and used to explain other relevant results. For instance, it can be used to explain certain results related to the controversial problem of SAWs on the critical percolation clusters. More particularly, if one accepts that $\nu$ on the backbone of the infinite percolation cluster is definitely larger than 3/4 [17, 18] and looks for possible reasons for such a conclusion, then our result ($b_h = 26$) offers an explanation. Namely, the conclusion originates from the MC simulations on backbones (see figure 1 of reference [17]) which appear to be finitely ramified fractals with homogeneous parts of the size $b_B \lesssim 10$, that is, with $b_B < b_h$ and which, on the grounds of our results, should have $\nu > 3/4$.

## Acknowledgments

## References

[1]   Elezović S, Knežević M and Milošević S 1987 *J. Phys. A: Math. Gen.* **20** 1215
[2]   Milošević S and Živić I 1991 *J. Phys. A: Math. Gen.* **24** L833
[3]   Živić I, Milošević S and Stanley H E 1993 *Phys. Rev. E* **47** 2430
[4]   Elezović-Hadžić S and Milošević S 1992 *J. Phys. A: Math. Gen.* **25** 4095
[5]   Vicsek T 1983 *J. Phys. A: Math. Gen.* **16** L647
[6]   Given A G and Mandelbrot B B 1983 *J. Phys. B: At. Mol. Phys.* **16** L565
[7]   Redner S and Reynolds P J 1981 *J. Phys. A: Math. Gen.* **14** 2679
[8]   Dhar D 1988 *J. Physique* **49** 397
[9]   Rammal R, Toulouse G and Vannimenus J 1984 *J. Physique* **45** 389
[10]  Havlin S and Ben-Avraham D 1987 *Adv. Phys.* **36** 695
[11]  Aharony A and Harris A B 1989 *J. Stat. Phys.* **59** 1091
[12]  Bouchaud J P and Georges A 1989 *Phys. Rev. B* **39** 2846
[13]  Roy A K and Blumen A 1990 *J. Stat. Phys.* **59** 1581
[14]  Dekeyser R, Maritan A and Stella A 1987 *Phys. Rev. Lett.* **58** 1758
[15]  Huber G 1992 (unpublished)
[16]  Bubanja V, Knežević M and Vannimenus J 1993 *J. Stat. Phys.* **71** 1
[17]  Woo K Y and Lee S B 1991 *Phys. Rev. A* **44** 999
[18]  Vanderzande C and Komoda A 1992 *Phys. Rev. A* **45** R5335